

Attachment Chemistry of Organic Molecules on Si(111)-7 × 7

FENG TAO AND GUO QIN XU*

Department of Chemistry, National University of Singapore,
10 Kent Ridge, Singapore, 119260

Received February 9, 2004

ABSTRACT

Molecular attachment chemistry is emerging as an important approach to tailor the chemical, physical, and mechanical properties of silicon surfaces, as well as to incorporate organic functions into silicon-based devices for various technological needs. The chemical bonding and reactivity of various organic molecules on Si(111)-7 × 7 were systematically studied using XPS, HREELS, TPD, UPS, STM, and DFT calculations. The spatial arrangements and unique electronic properties of reactive adatoms and rest atoms on the surface offer rich attachment chemistry for organic functionalities. Investigations demonstrated that organic molecules can be chemically bound to Si(111)-7 × 7 through several reaction pathways, including [4 + 2]- and [2 + 2]-like additions, dative bonding, and dissociative reaction. This Account reviews the recent progress and current understanding of reactivity, selectivity, and mechanisms of organic molecules on Si(111)-7 × 7.

Introduction

In recent decades, microelectronics has grown into the heart of modern industries, driving almost all of the technologies of today. Silicon, the most technologically important material, plays ubiquitous and unreplaceable roles in the development of microelectronic computing, micro- and optoelectronic devices, microelectromechanical machines, three-dimensional memory chips, and sensitive silicon-based nano- or biological sensors. Studies on silicon-based devices and surface chemistry have received explosive attention.^{1–6}

One important motivation for exploring the silicon surface chemistry is to fine tune the electronic properties of silicon surfaces. Attaching molecules onto surfaces enables us to have the necessary control over the electron-transfer efficiency through interfaces.^{7,8} It provides a versatile and reproducible way to tailor the electronic properties of semiconductor surfaces in a controllable manner.^{9,10} Another driving force is to incorporate organic molecular properties, such as size and shape effects, absorption spectrum, flexibility, conductivity, chemical

affinity, chirality, and molecular recognition into existing silicon-based devices and developing biomedical sensors.³

Si(100) and Si(111)-7 × 7 are the two most important and well-understood crystallized silicon surfaces. In a 2 × 1 reconstructed surface of Si(100), adjacent Si atoms pair into dimers. The bonding within a surface dimer can be described in terms of a σ bond coupled with a weak π bond, analogous to the well-known C=C bond in organic chemistry. Systematic investigations showed that unsaturated organic molecules can be bonded to this surface through pericyclic additions, dissociative reactions, and other mechanisms.^{3–6}

Si(111)-7 × 7 is formed through a 7 × 7 reconstruction involving a layer-by-layer construction on a base layer with 49 silicon atoms of a (111) surface, reducing the number of 3-coordinated Si atoms from 49 to 19 in each unit cell. This construction is schematically represented in Figure 1a. As shown in the adatom layer (Figure 1a₄), adatoms are these atoms in the topmost layer and have dangling bonds protruding upward. Rest atoms are the six 3-coordinated Si atoms in the rest atom layer (labeled with red circles in Figure 1a₃). A total of 12 adatoms, 6 rest atoms, and 1 corner atom accounts for the 19 dangling bonds for each unit cell.^{11a} The detailed structure of Si(111)-7 × 7 was described by Takayanagi et al.^{11b} Figure 1b is the top view of Si(111)-7 × 7, showing the adatom, rest atom, and dimer layers.

The 19 dangling bonds are located at 7 spatially inequivalent types of Si atoms, namely, corner and center adatoms on both faulted and unfaulted halves, faulted and unfaulted rest atoms, and the corner-hole atom. Upon reconstruction, each rest atom or corner has a formal charge of -1 , while each adatom has an electron occupancy of only $5/12$, leading to a formal charge of approximately $+7/12$.¹² Furthermore, each center adatom has two neighboring rest atoms, but only one for each corner adatom. The amount of charge transferred from a center adatom to the rest atom is roughly twice as much as that from a corner adatom. Consequently, the corner adatom has a higher electron density of occupied states than the center adatom, implying their different reactivities. The inherent differences in the electron structure among these atoms are readily distinguishable in STM images (parts c and d of Figure 1).

It is evident that this surface provides a number of spatially and electronically inequivalent reactive sites. Because of the large difference in electron density among surface atoms containing dangling bonds, an adatom coupled with one adjacent rest atom can act as a strong dipole, making addition reactions of alkenes with Si(111)-7 × 7 possible, similar to the polar additions of unsaturated organic molecules with Si(100).^{4–6,13} For convenience, the reaction involving one C=C bond is termed as [2 + 2]-like addition. Similarly, it is called [4 + 2]-like addition if a conjugated diene participates.

* To whom correspondence should be addressed. E-mail: chmxuq@nus.edu.sg. Telephone: (65) 6874 3595. Fax: (65) 6779 1691.

Feng Tao was born in 1971 in China. He received his Master's degree from Sichuan University. From 1998 to 2002, he had worked on organic modification and functionalization of semiconductor surfaces with Professor Xu at the National University of Singapore.

Guo-Qin Xu graduated with a B.Sc. in chemistry from Fudan University in 1982. After receiving his Ph.D. from Princeton University in 1987, he worked as a research associate at Brookhaven National Laboratory and University of Toronto. In 1991, he joined the Department of Chemistry at the National University of Singapore. His research mainly focuses on semiconductor surface chemistry and nanomaterials. He received the Singapore Youth Award (Science and Technology) in 1997. Currently, he is a professor of chemistry and Vice Dean of Faculty of Science at the National University of Singapore.

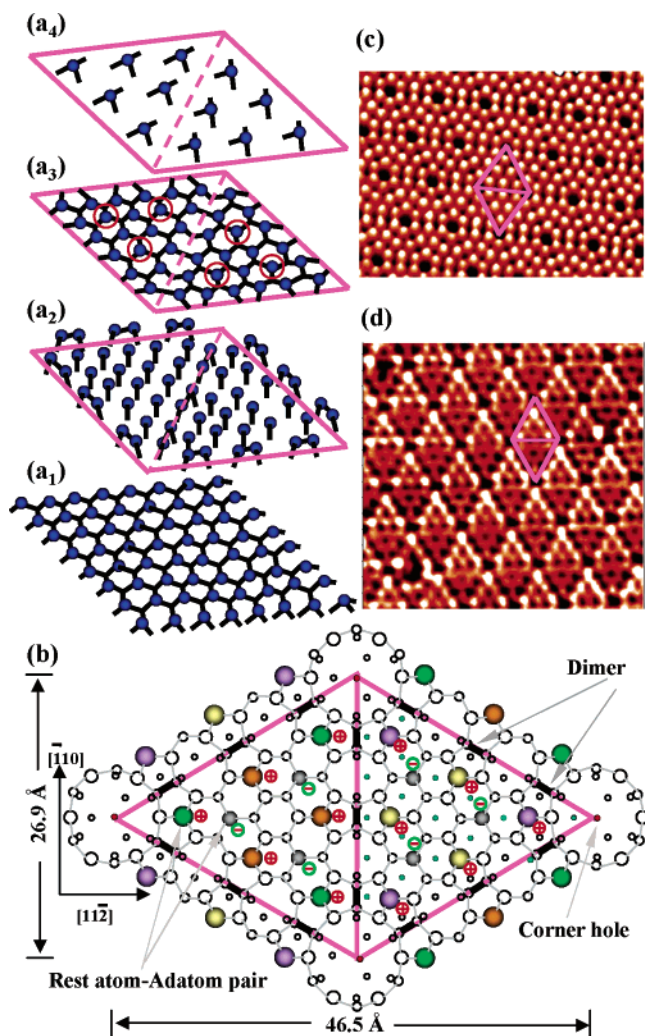


FIGURE 1. (a) Representation of layer-by-layer construction of the Si(111)- 7×7 structure. (a₁) Base layer, (1 \times 1) unstructured surface. (a₂) Dimer layer, the bottom layer of the reconstructed double layer. (a₃) Rest-atom layer, the second layer of the reconstructed double layer. (a₄) Adatom layer. More details are in ref 11a. (b) Top view of the 3D structure of the Si(111)- 7×7 unit cell. (c) and (d) STM image of unoccupied and occupied states of Si(111)- 7×7 , respectively. Pink triangular box represents a half unit cell.

Because of the existence of multiple reactive sites, Si(111)- 7×7 is expected to display diversities of reaction mechanisms for different organic molecules. To obtain new insight into a wide range of surface organic reactions, our group has concentrated on investigating the attachment chemistry of organic molecules on Si(111)- 7×7 in the last several years.¹⁴ From the viewpoint of surface chemistry research, we made efforts to elucidate the nature of chemisorption of organic molecules on this surface. For practical application in fine-tuning chemical, physical, and electronic properties of silicon surfaces, we were interested in exploring new approaches to create various well-defined organic/silicon interfaces for further fabricating organic molecular architectures.

The studies were carried out using various experimental techniques¹⁵ and theoretical approaches. High-resolution electron energy loss spectroscopy (HREELS) is

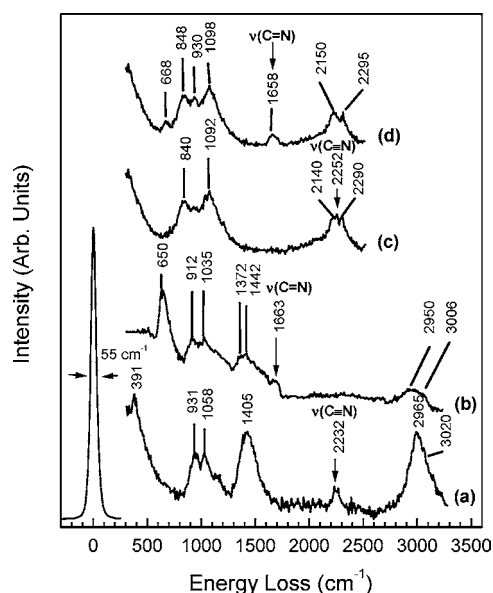


FIGURE 2. Vibrational features of adsorbed CH₃CN or CD₃CN on Si(111)- 7×7 . (a) and (b) are the physisorbed and chemisorbed CH₃CN, respectively. (c) and (d) are the physisorbed and chemisorbed CD₃CN, respectively.

the main technique used to characterize the vibrational signatures of adsorbed molecules on Si(111)- 7×7 . The core levels and valence band structures of the organic layer on this surface were studied using X-ray/ultra-violet photoelectron spectroscopies (XPS and UPS). Binding sites were investigated with scanning tunneling microscopy (STM). Density functional theory (DFT) was commanded to calculate the binding energies and predict the configurations of molecules chemisorbed on Si(111)- 7×7 . This review focuses on the latest understanding of the reactivity and selectivity of various organic molecules on Si(111)- 7×7 .

[2 + 2]-like Addition Chemistry

In organic chemistry, C=C, C≡C, and C≡N are three of the basic units for building organic molecules. The early studies implied that Si(111)- 7×7 displays a high reactivity for ethylene^{16a} and acetylene.^{16b} Subsequent investigations proved that the adjacent adatom–rest-atom pair of Si(111)- 7×7 can act as a *di*-radical to react with ethylene and acetylene to form two Si–C σ bonds.^{17,18} The covalent binding and thermal decomposition of some CN-containing molecules were also studied.^{14a,19} Being one prototype of organic molecules containing polarized unsaturated functionality, acetonitrile is chosen as an example to illustrate the binding mechanism.^{14a}

Figure 2 presents the HREELS spectra of physisorbed and chemisorbed CH₃CN and CD₃CN on Si(111)- 7×7 . Compared to physisorbed CH₃CN (Figure 2a), the vibrational feature of $\nu_{\text{C}\equiv\text{N}}$ around 2232 cm⁻¹ is absent in the chemisorbed acetonitrile. In addition, a shoulder appears around 1550–1700 cm⁻¹, which is close to the vibrational peak of CH₃ bending and attributable to the stretching mode of the C=N bond in chemisorbed molecules. The assignment of $\nu_{\text{C}\equiv\text{N}}$ was further confirmed in the study of

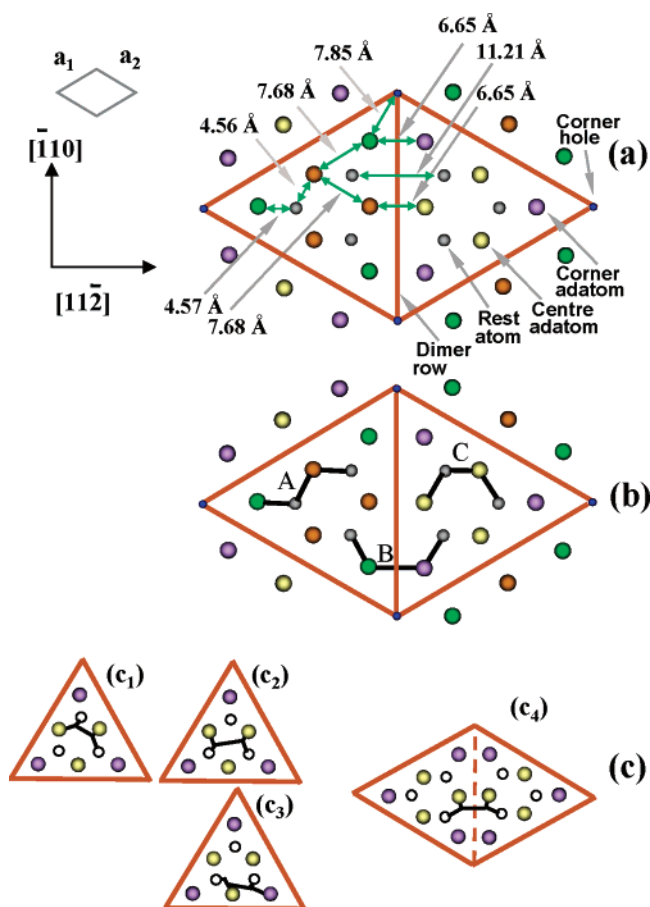


FIGURE 3. (a) Arrangement and separation of reactive adatoms, rest atoms, and corner holes in a Si(111)-7 × 7 unit cell. (b) Three modes (A, B, and C) of two adjacent *neighboring adatom–rest-atom pairs* in a unit cell. (c) Representation of four binding configurations of 1,6-heptadiene on Si(111)-7 × 7 revealed by STM.²⁰

CD₃CN by the well-resolved peak at ~1658 cm⁻¹ (Figure 2d). On the other hand, the C 1s and N 1s core levels of the CN group downshift respectively by 2.2 and 1.3 eV, suggesting their direct participation in chemical binding. Thus, both the vibrational and electronic evidences demonstrate that acetonitrile is covalently attached to Si(111)-7 × 7 with both Si–C and Si–N covalent bonds via a [2 + 2]-like addition.

On the basis of the polarization of the C≡N group, the configuration with N atom binding to an adatom and the C atom to an adjacent rest atom seems to be favorable. DFT calculations indeed showed that the reversed binding order (N atom to a rest atom) is thermodynamically preferred, minimizing the steric repulsion.

A similar [2 + 2]-like addition mechanism was also found for cyclohexene^{14b} and some unconjugated dienes²⁰ on Si(111)-7 × 7. For 1,7-octadiene, because of its large molecular size and two available unconjugated C=C bonds, it forms four σ bonds with two *neighboring adjacent adatom–rest-atom pairs* via two [2 + 2]-like additions.²⁰ In Figure 3b, A, B, and C are three possible modes for this *tetra-σ* adduct. Similar binding involving more than one adjacent adatom–rest-atom pairs was also

observed for chemisorbed 1,6-heptadiene and other dienes on this surface by STM.²⁰ Figure 3c represents four configurations of 1,6-heptadiene covalently bonded to two adatom–rest-atom pairs of Si(111)-7 × 7 revealed with STM.

[4 + 2]-like Chemical Binding of Nonaromatic Molecules

On the basis of the [2 + 2]-like addition mechanism of acetonitrile,^{14a} acetylene,¹⁸ and ethylene¹⁷ on Si(111)-7 × 7, molecules containing conjugated diene-like functionalities possibly bond to this surface through a [2 + 2]-like and/or [4 + 2]-like addition. Acrylonitrile, a typical heteroatomic conjugated diene, was considered as a model to demonstrate the reactivity and selectivity of multifunctional nonaromatic molecules on Si(111)-7 × 7.^{14d} It may possibly bind to Si(111)-7 × 7 with C=C or C≡N through [2 + 2]-like addition or C=C–C≡N via [4 + 2]-addition.

Figure 4 shows the vibrational features of acrylonitrile-2-*d*₁ on Si(111)-7 × 7. The C³–H stretching peak shifts from 3101 and 3002 cm⁻¹ for physisorbed molecules to 2935 cm⁻¹ for the chemisorbed state, demonstrating the rehybridization of the C³ atom from sp² to sp³. Another major change is the appearance of a new peak at 2028 cm⁻¹ upon chemisorption, ascribed to the characteristic vibration of a C²=C¹=N skeleton.²¹ These vibrational signatures lead to the conclusion that acrylonitrile covalently bonds to an adjacent adatom–rest-atom pair via the [4 + 2]-like addition, further confirmed by XPS and UPS studies.

The energies of possible chemisorbed configurations were calculated using SPARTAN at the DFT theory level of pBP86/DN** (comparable 6–31 G**).²² As shown in the bottom-left panel of Figure 5, Cluster II (Si₃₀H₂₈) was cut from the central part of MMFF94-optimized Cluster I containing 973 atoms. A further reduction in size gives Cluster III (Si₉H₁₂), serving as the mother cluster for the DFT calculation. Calculation results showed that the [4 + 2]-like adduct is the most stable product, where the N and C³ atoms are linked to the adjacent adatom and rest-atom pair, respectively, forming a H₃C³–C²H=C¹=NH-like structure.

The selective binding of acrylonitrile can be rationalized with the combined effects of electronic properties and geometries of the participating organic functionality and surface reactive sites. As was well-documented, the reactive sticking probabilities of cyclopentene on Si(100) (1.0),²³ Ge(100) (0.1),²³ and C(100) (0.001),²⁴ closely correlate with the extent of surface dimer buckling. The dimers on Si(100) and Ge(100) were experimentally and theoretically shown to be buckled.^{25a–c} However, no buckled dimers are present on C(100).^{25b,c} The electron transfer from the “down” atom to the “up” atom of a dimer results in the polarization of Si=Si and Ge=Ge dimers, making the buckled-down atom electrophilic and buckled-up atom nucleophilic.^{23,25a–c} These analyses demonstrate that the polarization of surface sites significantly

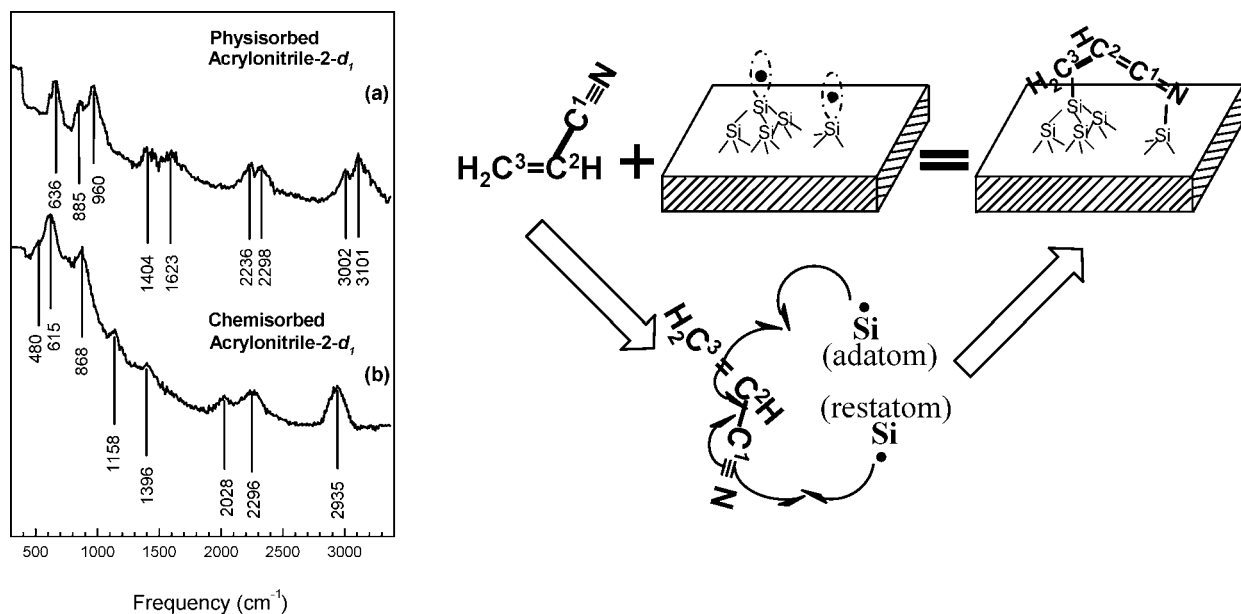


FIGURE 4. Vibrational features of physisorbed (a) and chemisorbed (b) acrylonitrile-2- d_1 on Si(111)- 7×7 . The right panel is the reaction scheme between acrylonitrile and this surface.

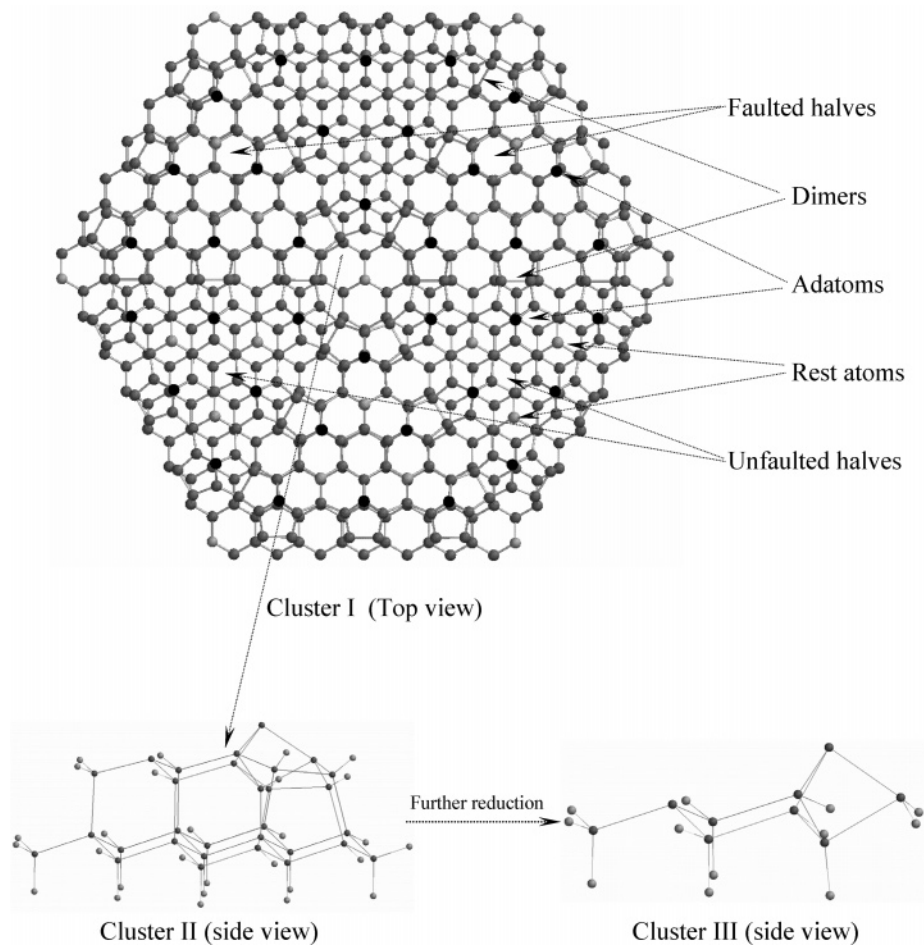


FIGURE 5. Clusters used for calculation of organic molecules chemisorbed on Si(111)- 7×7 .

enhances its reactivity with the C=C group of organic molecules.²⁴

A similar approach may also be employed to understand the selectivity of reaction channels for acrylonitrile

on Si(111)- 7×7 . Among the three reactive groups including $C^3=C^2$, $C^1\equiv N$, and $C^3=C^2-C^1\equiv N$, the larger polarity of $C^1\equiv N$ or $C^3=C^2-C^1\equiv N$ makes it *both* electrophilic and nucleophilic. Thus, a lower transition state is expected

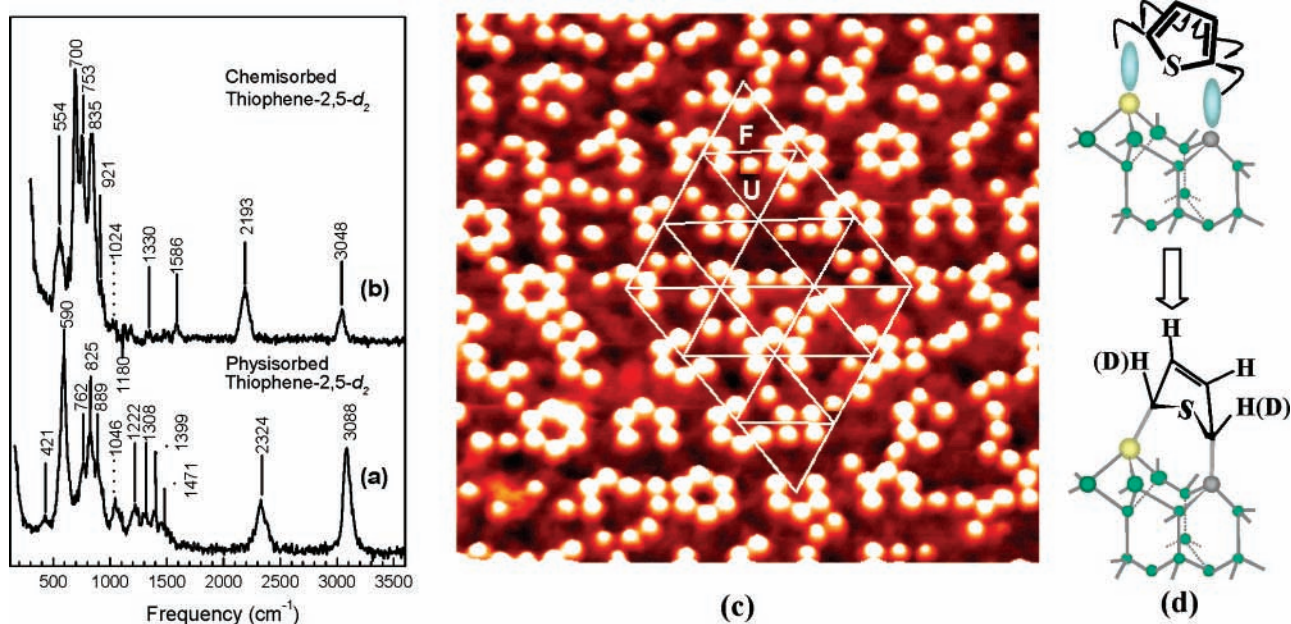


FIGURE 6. Physisorbed (a) and chemisorbed (b) thiophene-2,5- d_2 on Si(111)- 7×7 . (c) STM images ($\sim 160 \times 160 \text{ \AA}$, $V_s = 1.7 \text{ V}$) of chemisorbed thiophene on Si(111)- 7×7 . (d) Reaction scheme of thiophene on Si(111)- 7×7 .

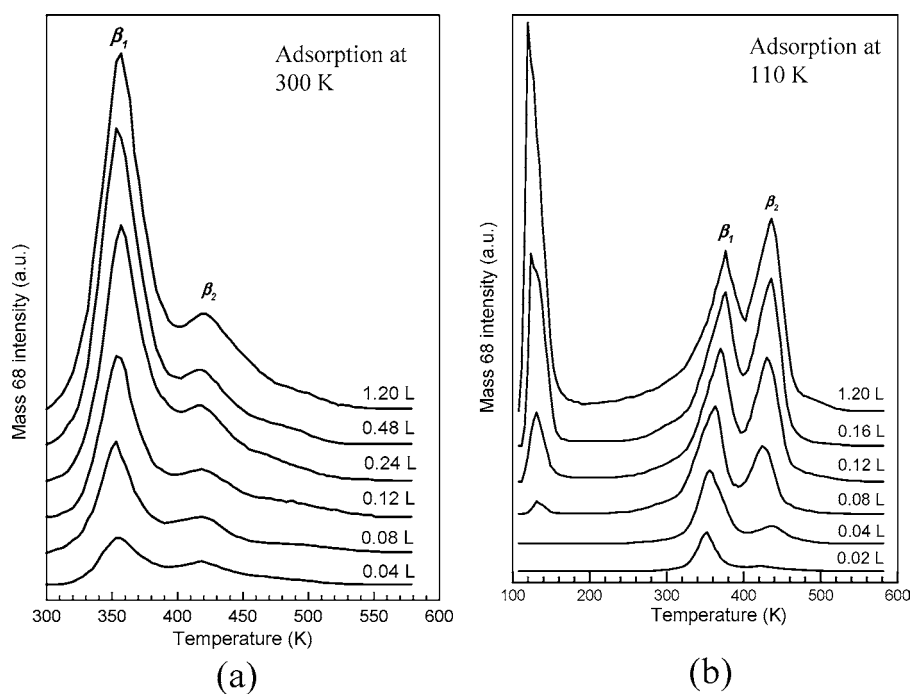


FIGURE 7. TPD spectra of furan ($m/z = 68$) as a function of the furan exposure at 300 K (a) and at 110 K (b).

for the addition between the polar $C^3=C^2-C^1\equiv N$ or $C^1\equiv N$ and the neighboring adatom–rest-atom pair. On the other hand, the geometrical matching between the adjacent adatom–rest-atom pair and the dimension of the reactive group may also have a significant influence on the competition and selectivity of different reaction channels. The (Si) C^3-C^2 (Si) or (Si) $C^1=N$ (Si) distance in the possible [2 + 2]-like adduct is obviously smaller than the separation of 4.5 \AA between an adatom and its adjacent rest atom, thereby resulting in a large strain in its product. However, the dimension of

(Si) $C^3H_2-C^2H=C^1=N$ (Si) of the [4 + 2]-like adduct matches well with the surface reactive sites. This understanding is consistent with the preferred [4 + 2]-like addition from both experimental evidences and DFT calculations. Because of the small difference in adsorption energies, the issue related to two possible configurations of the [4 + 2]-like adduct corresponding to the nitrogen atom terminated either at an adatom or at a rest atom still remains open. A similar reaction mechanism was also demonstrated for 1,3-cyclohexadiene^{14b} and 1,3-butadiene²⁶ on Si(111)- 7×7 .

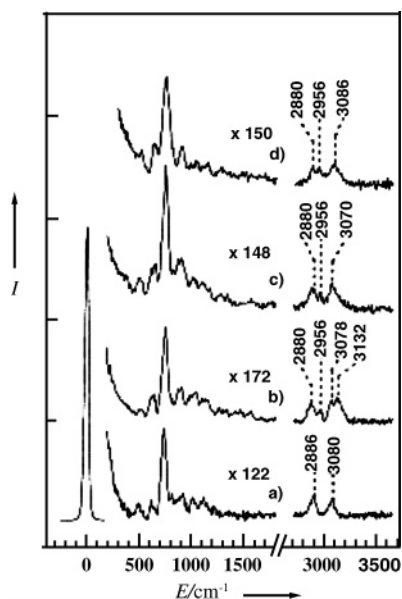


FIGURE 8. Vibrational spectra obtained after exposing 1.20 L of furan to Si(111)-7 \times 7 (a) at 300 K, (b) at 110 K, (c) after annealing the sample from b to 300 K, and (d) after annealing the sample from b to 360 K.

[4 + 2]-like Addition Scheme for Aromatic Molecules

The attachment chemistry of benzene on Si(111)-7 \times 7 has been extensively studied. The earlier work suggested adsorption via a π interaction.²⁷ However, recent investigations using HREELS with a higher resolution^{14e} and DFT calculations²⁶ demonstrated a covalent *di*- σ -binding mode through a [4 + 2]-like addition strategy. This was further confirmed in other aromatic systems including thiophene, furan, and chlorobenzene.^{14f-h} In this Account, the binding of thiophene to Si(111)-7 \times 7 is chosen to exemplify the covalent attachment of aromatic molecules.^{14f}

In Figure 6, the vibrational loss at 2324 cm^{-1} associated with the (sp^2) $\text{C}^{2,5}$ -D stretching mode of physisorbed thiophene-2,5- d_2 is seen to downshift to 2193 cm^{-1} assigned to the (sp^3) C-D stretching in chemisorbed molecules. Such a shift was not detected for (sp^2) $\text{C}^{3,4}$ -H stretching, showing that both C^3 and C^4 maintain sp^2 hybridization upon chemisorption. Thus, these experimental observations provide clear evidences for the involvement of the C^2 and C^5 atoms of thiophene in the bond formation with Si(111)-7 \times 7.

Statistical counting of STM images at low coverage indicates that the reactivity of center adatoms is about 2 times that of the corner adatoms, and the reaction prefers the adatoms in faulted subunits over those in unfaulted halves with a ratio of 2.4:1. The saturation coverage of chemisorbed thiophene (defined as the ratio between the reacted adatoms and the total Si atoms, 49 at the base layer) (Figure 6c) was estimated to be about 0.13 monolayer at room temperature, giving an average of 6 adatoms per unit cell participating in the reaction with thiophene. Furthermore, the equal number (6) of reacted adatoms to rest atoms per unit cell strongly suggests that one thiophene molecule binds to one adjacent adatom-rest atom pair.

These experimental findings unambiguously showed that the adjacent adatom and rest atom can serve as a *di*-radical for the [4 + 2]-like addition with thiophene, forming a 2,5-dihydrothiophene-like structure (Figure 6d). A similar binding mode was also found for chemisorbed chlorobenzene on Si(111)-7 \times 7.^{14g}

Dangling-Bond-Mediated Dimerization of Furan

Experimental and theoretical studies suggested that the Si dangling bonds of adjacent adatom-rest atom pairs can be viewed as reactive "*di*-radicals" in the surface attachment of aromatics to form Si-C σ bonds.^{14e-g} On the other

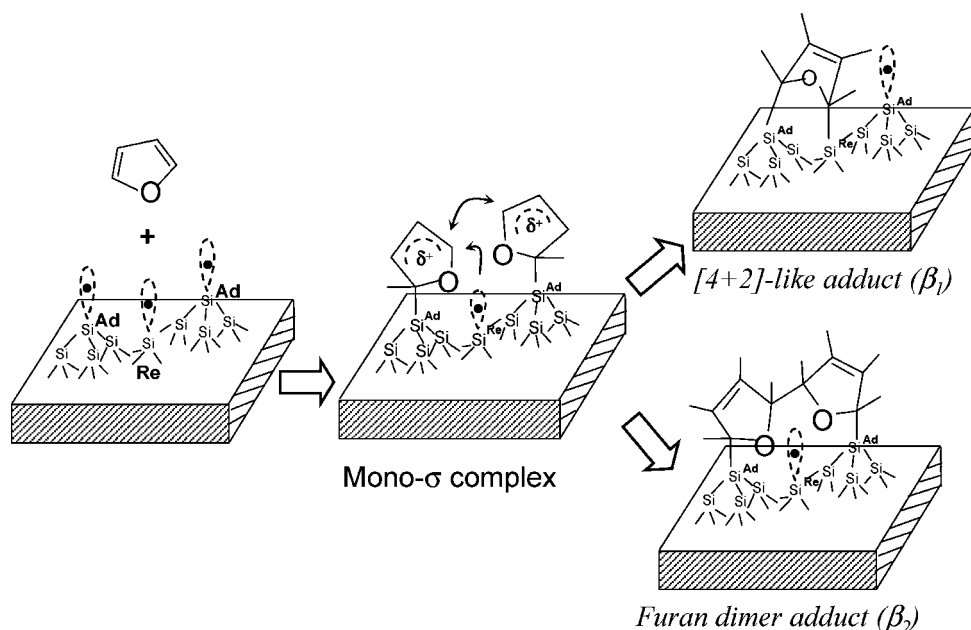


FIGURE 9. Scheme of reaction mechanisms for furan on Si(111)-7 \times 7 to form the [4 + 2]-like adduct and dimerized furan complex.

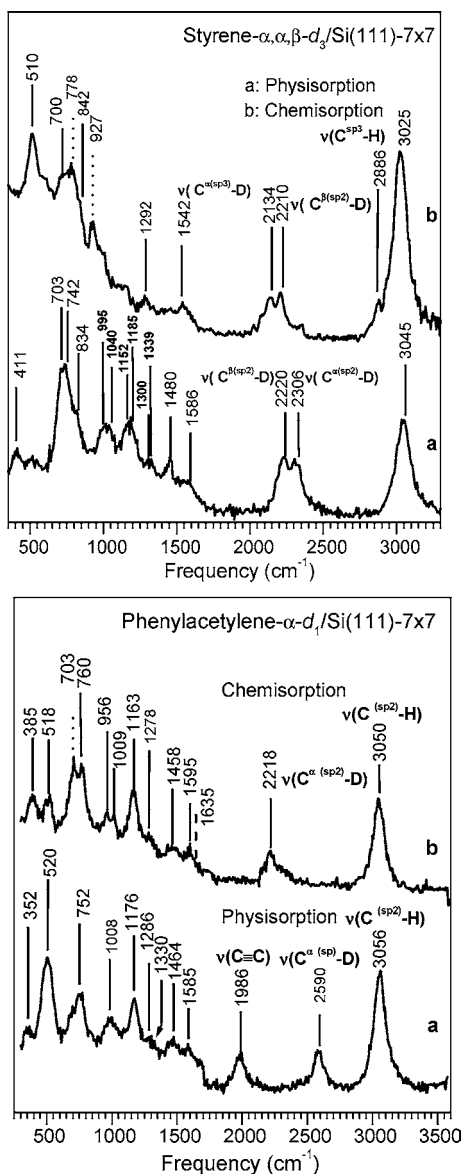


FIGURE 10. Vibrational spectra of physisorbed and chemisorbed styrene- α,α,β - d_3 and phenylacetylene- α - d_1 on Si(111)-7 \times 7.

hand, organic radical-based C–C bond formation in solution is highly selective in enantioselective synthesis²⁸ and the preparation of controlled macromolecular architectures.²⁹ Therefore, it is of significant interest to investigate whether this radical-based C–C coupling is feasible on silicon surfaces in association with the radical behavior of silicon dangling bonds. Such a study may open a new door for dry organic syntheses on silicon surfaces. Indeed, experimental evidences from temperature-programmed desorption (TPD) and HREELS showed silicon dangling-bond-mediated dimerization of furan molecules on Si(111)-7 \times 7.^{14h}

TPD spectra of furan obtained after various initial exposures of furan at 300 K are displayed in Figure 7a. Two chemisorption states can be found at 360 K (β_1) and 420 K (β_2). The population of the β_2 state remains very low even at the saturation exposure. However, the TPD spectra collected at 110 K are quite different (Figure 7b). At low exposures, the desorption profiles are identical to

those obtained after exposures at 300 K, with β_1 being the major state. As increasing furan exposure, the population of the β_2 peak grows much faster. Upon saturation, the β_2 becomes the dominant feature. This surprising change in the relative intensities of the β_1 and β_2 peaks as a function of adsorption temperatures suggests the formation of a unique chemisorption state, further confirmed by the vibrational evidence.

Figure 8a is the HREELS spectrum taken after exposing furan to Si(111)-7 \times 7 at 300 K. Two separate vibrational features at 2886 cm^{-1} (sp^3 C–H) and 3080 cm^{-1} (sp^2 C–H) indicate the rehybridization in the chemisorbed furan. The overall features in Figure 8a are in good agreement with a [4 + 2]-like adduct assigned to the predominant β_1 state at 300 K. Figure 8c shows the combined vibrational features contributed from the β_1 and β_2 states but without physisorbed molecules. Three vibrational features at 3070, 2956, and 2880 cm^{-1} of C–H stretching modes can be resolved. Compared to the spectrum obtained by adsorbing molecules at 300 K (Figure 8a), in which the β_1 state predominates, it is concluded that the additional weak feature at 2956 cm^{-1} arises from the β_2 state.

When the sample exposed to 1.20 L of furan at 110–360 K is progressively annealed, only the β_2 state of chemisorbed furan is retained on Si(111)-7 \times 7 (Figure 8d). The presence of the sp^3 C–H stretching peaks at both 2956 and 2880 cm^{-1} suggests the existence of two types of sp^3 -hybridized carbon atoms in the more strongly bonded β_2 state.

According to the stepwise *di*-radical mechanism, the initial molecular adsorption leads to the formation of a *mono*- σ -bonded surface complex (Figure 9) involving a linkage between the electron-rich α -carbon atom in furan and the electron-deficient Si adatom site. At room temperature, the radical-like precursor state readily reacts with a nearby rest atom, leading to the predominant formation of the β_1 state corresponding to a [4 + 2]-like adduct. However, at 110 K, the *mono*- σ -bonded precursor state is thermally stabilized and a high population of this state can be built up on the surface. Two *mono*- σ -bonded species resting on two adjacent adatoms can readily recombine to form a new C–C bond. This recombinative reaction leads to the formation of a covalently C–C-linked, dimer-like furan adsorption complex through C $^\alpha$ –C $^\alpha$ coupling (Figure 9). In the dimerized complex (β_2), the chemical environment of the two C–C-linked α -carbon atoms is clearly different from that of carbon atoms directly bonded to the silicon atoms, resulting in two resolvable C $^{\text{sp}3}$ –H stretching peaks at 2956 and 2880 cm^{-1} .

Influence of Substitution Groups on Reaction Mechanisms of Aromatic Systems

As is well-known, the external functionalities of substituted aromatic systems can significantly affect the electronic and chemical properties of aromatic systems through both inductive and resonance effects. Thus, investigating the

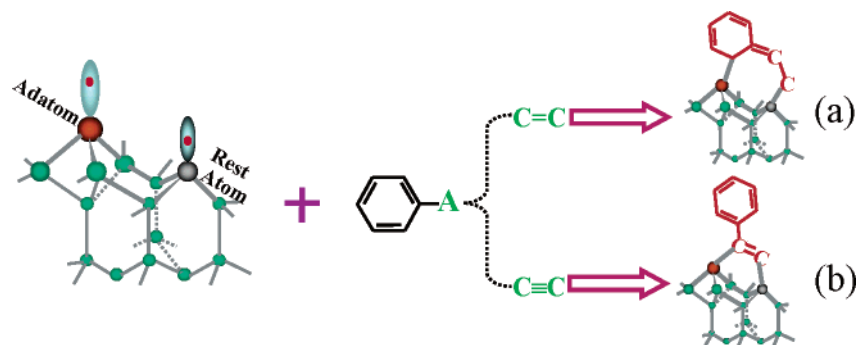


FIGURE 11. Schematic presentation for the adducts of styrene (a) and phenylacetylene (b) on Si(111)-7 \times 7 through [4 + 2]-like and [2 + 2]-like addition mechanisms, respectively.

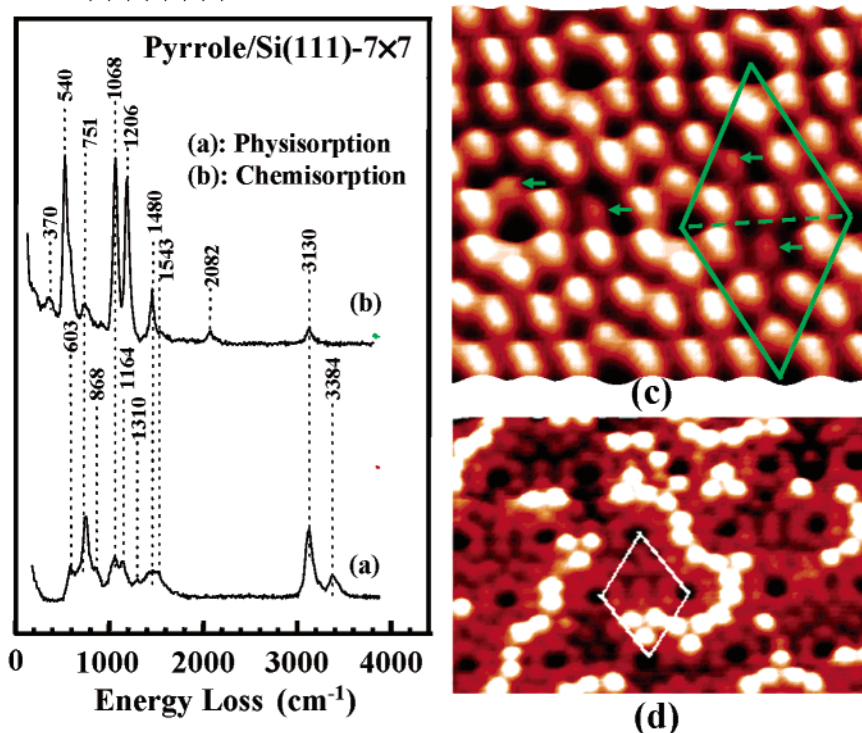


FIGURE 12. Vibrational spectra of physisorbed (a) and chemisorbed (b) pyrrole on Si(111)-7 \times 7. (c) STM images of the unoccupied state for low-exposure pyrrole molecules on Si(111)-7 \times 7 at a sample bias of 1.47 V. (d) Unoccupied state image at a sample bias of +3.2 V, corresponding to the formation of a chainlike nanostructure of pyrrole.

influence of substitution functionality on the selectivity and reactivity of aromatic molecules can mechanically direct chemical reactions to take place at a specific moiety of the molecular system.¹⁴ⁱ

Styrene is a representative π -conjugated phenyl-substituted molecule. It may covalently bond to Si(111)-7 \times 7 through four types of binding modes including addition reactions occurring at (i) one C=C bond of the phenyl ring, (ii) the external C=C bond, (iii) two conjugated C=C bonds of the phenyl ring, and (iv) both external C=C and its neighboring C=C of the phenyl ring.

In Figure 10, the peak at 2306 cm⁻¹ (C^{sp2}-D of =C ^{α} D₂ group) observed for physisorbed styrene- α,α,β -d₃ disappears upon chemisorption. This is accompanied by the appearance of a resolvable peak around 2886 cm⁻¹ attributed to C^{sp3}-H stretching, clearly showing the rehybridization of one or more carbon atoms of the phenyl

ring from sp² to sp³. These results support that styrene covalently binds to Si(111)-7 \times 7 through the [4 + 2]-like addition involving both the ethenyl group and its neighboring C=C of the phenyl ring, producing a 5-ethylidene-1,3-cyclohexadiene-like species, well consistent with DFT calculations.

Replacing the substitution group of C=C by a C \equiv C converts the molecule from styrene into phenylacetylene. Similar to styrene, it has four possible reaction channels. For chemisorbed phenylacetylene- α -d₁ (Figure 10), the vibrational features of (1) the disappearance of both C^{sp}-D and C \equiv C stretching modes, (2) the absence of C^{sp3}-H stretching, and (3) the preservation of characteristic vibrational modes of the *mono*-substituted phenyl ring unambiguously exclude the possibilities of attachment other than the formation of the styrene-like product (Figure 11b), confirmed by DFT prediction.

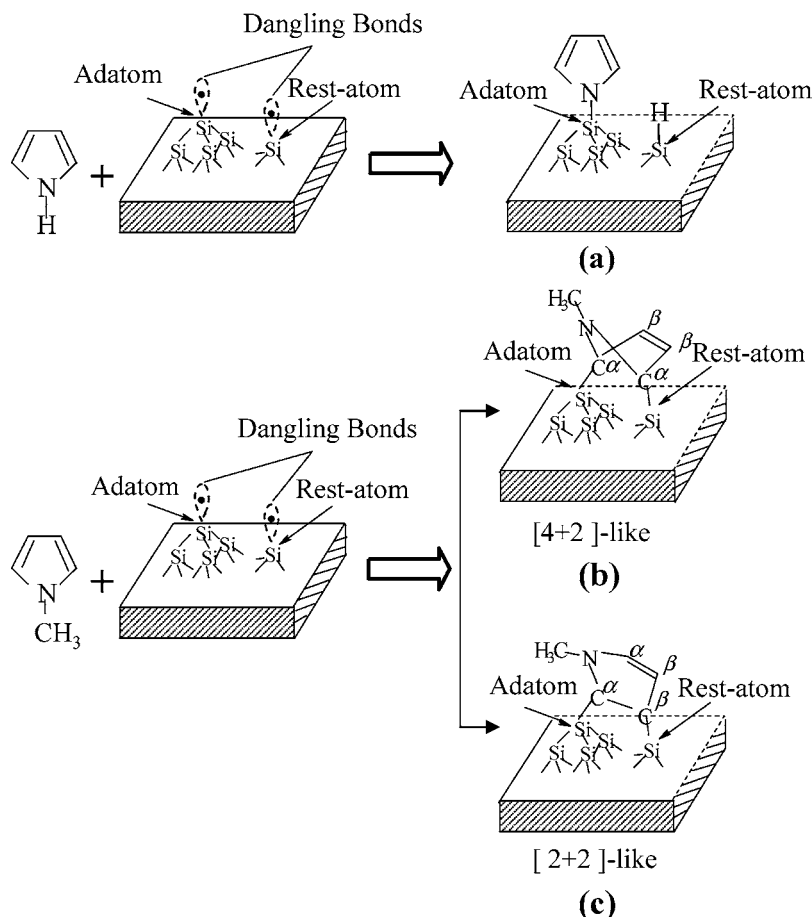


FIGURE 13. Scheme of dissociated products of pyrrole (a) and [4 + 2]-like adduct (b) and [2 + 2]-like adduct (c) of *N*-methylpyrrole on Si(111)-7 × 7.

Studies on the covalent attachment of benzene on Si(111)-7 × 7 revealed that benzene bonds to the adjacent adatom and rest-atom pair involving two conjugated unsaturated bonds.^{14e} For styrene, there are three possible addition pathways involving two conjugated C=C bonds. Among them, only the reaction via both the external C=C and its conjugated C=C of the phenyl ring can form a product containing three cumulative conjugated C=C bonds (Figure 11a), which was theoretically expected to have a lower energy than the other adducts. In the case of phenylacetylene, the *di*- σ bonding through [2 + 2]-like addition at the C≡C produces a highly conjugated styrene-like structure with the lowest energy. In addition, the higher reactivity of C≡C than C=C in electrophilic addition also contributes to the preferred [2 + 2]-like addition at C≡C of phenylacetylene. Indeed, a similar reaction channel to phenylacetylene was also observed for benzonitrile on Si(111)-7 × 7.^{14j}

Competition of Dissociative Reaction with Associative [4 + 2]-like and/or [2 + 2]-like Additions in Unsaturated Molecules

When pyrrole is compared to other aromatic molecules, including benzene, pyridine, thiophene, and furan, pyrrole has a hydrogen-terminated nitrogen, suggesting the possible competition of dissociative reaction at N–H with [4 + 2] and/or [2 + 2]-like addition. The attachment chem-

istry of pyrrole on Si(111)-7 × 7 was investigated to understand the competition and selectivity between these two possible reaction mechanisms.^{14k}

From the spectrum of chemisorbed pyrrole (Figure 12b), it is evident that the N–H stretching at 3384 cm⁻¹ observed for the physisorbed molecule is absent, consistent with the observation of Si–N bending and stretching at 370 and 540 cm⁻¹ and Si–H stretching at 2082 cm⁻¹. These vibration features demonstrate that pyrrole chemisorbs dissociatively on Si(111)-7 × 7 with the N–H bond cleavage.

DFT calculations showed that the dissociative product has a higher binding energy by 24–31 kcal mol⁻¹ than the 2,5-dihydropyrrole-like adduct formed via a [4 + 2]-like addition. This result is rather reasonable if one considers the retention of aromaticity in the dissociative channel in contrast to the breakage of aromaticity in the [4 + 2]-like addition. Furthermore, the calculation results also suggested that pyrrolyl binding at an adatom (Figure 13a) is sterically more favorable than attaching pyrrolyl to a lower-lying rest atom, where the ring may experience some repulsive interaction with the neighboring adatoms.

The specific chemisorption geometry was investigated with STM. Figure 12c presents a topographic image of unoccupied states of Si(111)-7 × 7 after a low exposure of pyrrole. As shown with a green-line box, the 7 × 7 reconstruction is still preserved upon chemisorption. How-

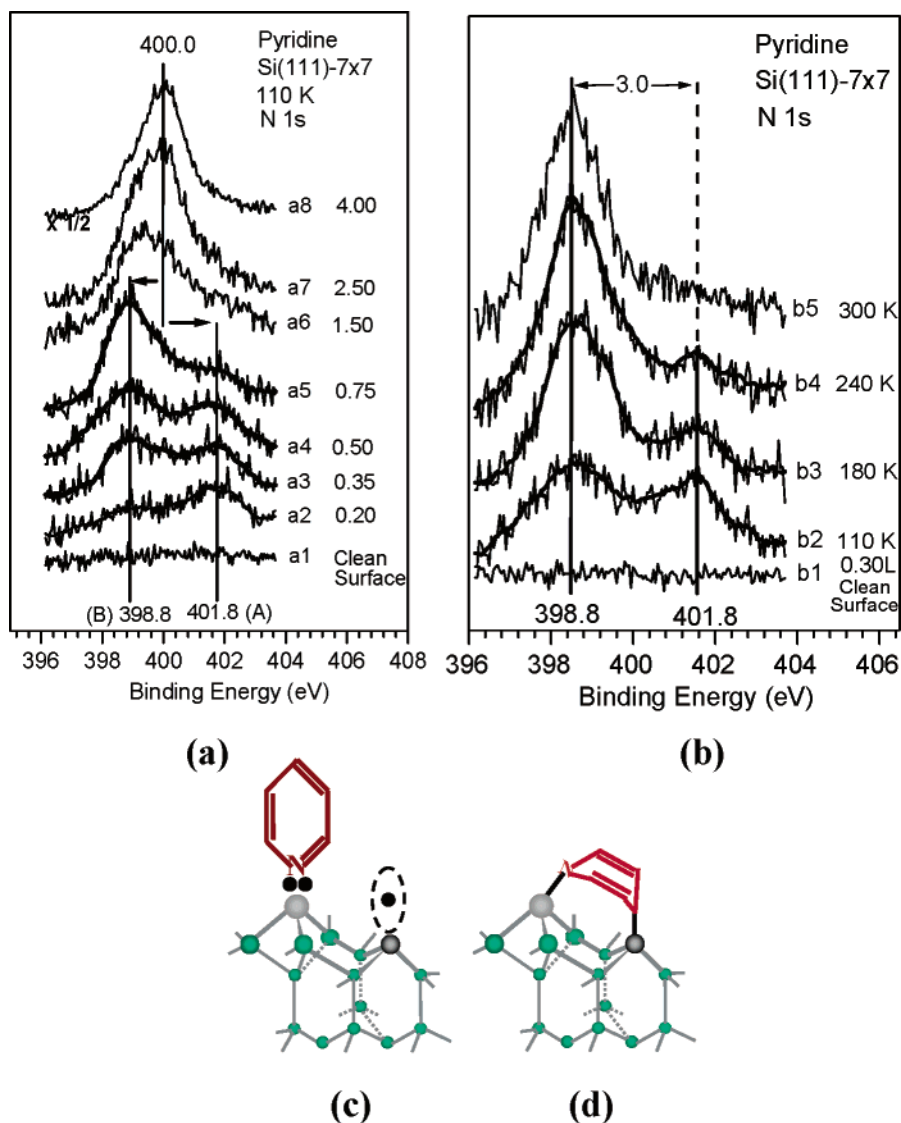


FIGURE 14. (a) N 1s binding energy for pyridine on Si(111)-7 \times 7 as a function of the exposure at 110 K. (b) N 1s binding energy for pyridine on Si(111)-7 \times 7 as a function of the temperature. (c) Schematic structure for state A. (d) Schematic structure for state B.

ever, the chemical attachment of pyrrole molecules causes some adatoms labeled with arrows to become dim, attributable to the consumption of their dangling bonds by covalent bonding with adsorbates. It is known that the H atom binding to an adatom of Si(111)-7 \times 7 gives a distinct STM feature, appearing like a missing adatom.^{30a} Thus, the dim but still visible adatom sites observed upon pyrrole chemisorption can be attributed to the binding of pyrrolyl radicals. This also implies the binding of H atoms to rest atoms adjacent to the dim adatoms, supported by the analyses of line profiles of the image in Figure 12c.^{14k} This is consistent with the previous STM study^{30b} and DFT calculation,^{30c} which showed that H atoms passivate preferentially the rest-atom sites because of the higher binding energy by 0.2 eV than that of the adatoms.

The chainlike or cluster features of adsorbed pyrrolyl were clearly observed in the empty-state image (Figure 12d), possibly attributed to the existence of an attractive interaction between the adsorbed pyrrolyl rings and the incoming gaseous pyrrole molecules. The greater contri-

bution of unoccupied molecular orbitals at high sample bias such as +3.2 V possibly results in the bright spots of chemisorbed pyrrolyl on Si(111)-7 \times 7.

The dissociative nature of pyrrole adsorption demonstrates that the N-H group is more reactive than the aromatic ring, forming a pyrrolyl-like skeleton. However, replacing the N-bonded H atom by methyl in *N*-methylpyrrole can alter its reaction pathway.^{14l} Experimental evidence showed that *N*-methylpyrrole covalently binds to Si(111)-7 \times 7 through both [4 + 2]-like and [2 + 2]-like additions (parts b and c of Figure 13). Thus, the selectivity of reaction channels for pyrrole and *N*-methylpyrrole demonstrates the possibility of switching reactions into the desired channel by slightly modifying molecular structures.

Formation of Dative Bond at the Organic/Semiconductor Interface

The largely uneven distribution of electron density at adatoms and rest atoms makes them possibly function

respectively as electron acceptors and donors to form dative bonds with molecules. Recent study showed that trimethylamine can form a dative bond with this surface.³¹ Pyridine with the lone-pair electrons at its N atom not directly involved in aromatic π conjugation can also serve as an electron donor to form a dative bond with the electron-deficient adatom.^{14m}

Two photoemission features of pyridine on Si(111)-7 \times 7 at 110 K can be clearly resolved at 401.8 eV (state A) and 398.8 eV (state B) at exposures of ≤ 0.50 L in Figure 14a. The increase of exposure leads to the appearance of an N 1s peak at 400.0 eV, attributable to physisorbed molecules. When pyridine/Si(111)-7 \times 7 is annealed to 240 K, two peaks at 398.8 and 401.8 eV are preserved, further confirming the chemisorption nature of states A and B.

For state A, its N 1s core level of 401.8 eV is ~ 3.0 and 1.8 eV higher than those of state B and physisorbed pyridine, respectively. This unusually high binding energy is comparable to 401.6 eV of $[(\text{CH}_3)_4\text{N}]^+\text{Br}^-$.³² It is reasonable to conclude that state A possibly results from the significant electron transfer from the N atom of pyridine to the surface Si atom through the formation of a N \rightarrow Si dative bond.

In Figure 14b, the increase of temperature results in the decrease in the intensity at 401.8 eV but some growth of the 398.8 eV peak, suggesting that state A possibly converts into B with increasing temperature. This conversion possibly originates from the weakening of pyridine aromaticity because of the electron transfer from the N to Si atom and the availability of a radical-like rest atom at a suitable distance. The vibrational studies of pyridine-2- d_1 showed that state B is a [4 + 2]-like adduct bonded to the surface via both Si-N¹ and Si-C⁴ σ linkages. Parts c and d of Figure 14 schematically present the structures of states A and B. The formation of a dative bond provides an alternative strategy for attaching organic molecules to Si(111)-7 \times 7.

Summary

These systematic studies demonstrated that organic functionalities can be chemically attached onto Si(111)-7 \times 7 through various reaction mechanisms including [2 + 2]-like and [4 + 2]-like additions, dative bonding, and dissociative reaction. The resulting organic monolayers on silicon surfaces containing reactive functionalities can be employed as templates to develop molecular architectures, as well as for further organic modification and functionalization of the silicon surface. When desirable functional molecules are chosen, chirality, molecular recognition, biosensitivity, conductivity, or nonlinear optical properties are expected to be incorporated into silicon-based devices and materials.

References

- (1) Maboudian, R. Surface Process in MEMS Technology. *Surf. Sci. Rep.* **1998**, *30*, 209–270.
- (2) Wong, H. S. P. Beyond the Conventional Transistor. *IBM J. Res. Dev.* **2002**, *46*, 133–168.
- (3) Yates, J. T. Surface Chemistry: A New Opportunity in Silicon-Based Microelectronics. *Science* **1998**, *279*, 335–336.
- (4) Wolkow, R. A. Controlled Molecular Adsorption on Silicon: Laying a Foundation for Molecular Devices. *Annu. Rev. Phys. Chem.* **1999**, *50*, 413–441.
- (5) (a) Hamers, R. J.; Coulter, S. K.; Ellison, M. D.; Hovis, J. S.; Padowitz, D. F.; Schwartz, M. P.; Greenlief, C. M.; Russell, J. N. Cycloaddition Chemistry of Organic Molecules with Semiconductor Surfaces. *Acc. Chem. Res.* **2000**, *33*, 617–624.
- (6) (a) Bent, S. F. Attaching Organic Layers to Semiconductor Surfaces. *J. Phys. Chem. B* **2002**, *106*, 2830–2842. (b) Bent, S. F. Organic Functionalization of Group IV Semiconductor Surfaces: Principles, Examples, Applications, and Prospects. *Surf. Sci.* **2002**, *500*, 879–903. (c) Filler, M. A.; Bent, S. F. The Surface as Molecular Reagent: Organic Chemistry at the Semiconductor Interface. *Prog. Surf. Sci.* **2003**, *73*, 1–56.
- (7) Haran, A.; Waldeck, D. H.; Naaman, R.; Moons, E.; Cahen, D. The Dependence of Electron-Transfer Efficiency on the Conformational Order in Organic Monolayers. *Science* **1994**, *263*, 948–950.
- (8) Moons, E.; Bruening, M.; Shanzer, A.; Beier, J.; Cahen, D. Electron Transfer in Hybrid Molecular Solid-State Devices. *Synth. Met.* **1996**, *76*, 245–248.
- (9) Lisensky, G. C.; Penn, R. L.; Murphy, C. J.; Ellis, A. B. Electrooptical Evidence for the Chelate Effect at Semiconductor Surfaces. *Science* **1990**, *248*, 840–843.
- (10) Monch, W. *Semiconductor Surfaces and Interfaces*. Springer: Berlin, Germany, 1995.
- (11) (a) Waltenburg, H. N.; Yates, J. T., Jr. Surface Chemistry of Silicon. *Chem. Rev.* **1995**, *95*, 1589–1673. (b) Takayanagi, K.; Tanishiro, T.; Takahashi, S.; Takahashi, M. Structural-Analysis of Si(111)-7 \times 7 by UHV-Transmission Electron-Diffraction and Microscopy. *J. Vac. Sci. Technol., A* **1985**, *3*, 1502–1506.
- (12) Northrup, J. E. Origin of Surface-States on Si(111)-(7 \times 7). *Phys. Rev. Lett.* **1986**, *57*, 154–157.
- (13) (a) Qiao, M. H.; Cao, Y.; Tao, F.; Liu, Q.; Deng, J. F.; Xu, G. Q. Electronic and Vibrational Properties of Thiophene on Si(100). *J. Phys. Chem. B* **2000**, *104*, 11211–11219. (b) Qiao, M. H.; Tao, F.; Cao, Y.; Li, Z. H.; Dai, W. L.; Deng, J. F.; Xu, G. Q. Cycloaddition Reaction of Furan with Si(100)-2 \times 1. *J. Chem. Phys.* **2001**, *114*, 2766–2774. (c) Tao, F.; Wang, Z. H.; Qiao, M. H.; Liu, Q.; Sim, W. S.; Xu, G. Q. Covalent Attachment of Acetonitrile on Si(100) through Si-C and Si-N Linkages. *J. Chem. Phys.* **2001**, *115*, 8563–8569. (d) Tao, F.; Wang, Z. H.; Xu, G. Q. Formation of a Benzimine-like Conjugated Structure through the Adsorption of Benzonitrile on Si(100). *J. Phys. Chem. B* **2002**, *106*, 3557–3563. (e) Tao, F.; Qiao, M. H.; Li, Z. H.; Yang, L.; Dai, Y. J.; Huang, H. G.; Xu, G. Q. Adsorption of Phenylacetylene on Si(100)-2 \times 1: Reaction Mechanism and Formation of A Styrene-like π -Conjugation System. *Phys. Rev. B* **2003**, *67*, 115334/1–7. (f) Qiao, M. H.; Cao, Y.; Deng, J. F.; Xu, G. Q. Formation of Covalent Si-N Linkages on Pyrrole Functionalized Si(100)-(2 \times 1). *Chem. Phys. Lett.* **2002**, *325*, 508–512.
- (14) (a) Tao, F.; Chen, X. F.; Wang, Z. H.; Xu, G. Q. Binding and Structure of Acetonitrile on Si(111)-7 \times 7. *J. Phys. Chem. B* **2002**, *106*, 3890–3895. (b) Tao, F.; Wang, Z. H.; Xu, G. Q. Covalent Binding of Cyclohexene, 1,3-Cyclohexadiene, and 1,4-Cyclohexadiene on Si(111)-7 \times 7. *Surf. Sci.* **2003**, *530*, 203–215. (c) Cao, Y.; Yong, K. S.; Wang, Z. H.; Deng, J. F.; Lai, Y. H.; Xu, G. Q. Cycloaddition Chemistry of Thiophene on the Silicon (111)-7 \times 7 Surface. *J. Chem. Phys.* **2001**, *115*, 3287–3296. (d) Tao, F.; Chen, X. F.; Wang, Z. H.; Xu, G. Q. Selective Formation of Cumulative Double Bonds (C=C=N) in the Attachment of Multifunctional Molecules on Si(111)-7 \times 7. *J. Am. Chem. Soc.* **2002**, *124*, 7170–7180. (e) Cao, Y.; Wei, X. M.; Chin, W. S.; Lai, Y. H.; Deng, J. F.; Bernasek, S. L.; Xu, G. Q. Formation of Di- σ Bond in Benzene Chemisorption on Si(111)-7 \times 7. *J. Phys. Chem. B* **1999**, *103*, 5698–5702. (f) Cao, Y.; Yong, K. S.; Wang, Z. Q.; Chin, W. S.; Lai, Y. H.; Deng, J. F.; Xu, G. Q. Dry Thienylation of the Silicon (111)-(7 \times 7) Surface. *J. Am. Chem. Soc.* **2000**, *122*, 1812–1813. (g) Cao, Y.; Deng, J. F.; Xu, G. Q. Stereo-Selective Binding of Chlorobenzene on Si(111)-7 \times 7. *J. Chem. Phys.* **2000**, *112*, 4759–4767. (h) Cao, Y.; Wang, Z. H.; Deng, J. F.; Xu, G. Q. Evidence for Dangling Bond Mediated Dimerization of Furan on the Silicon (111)-(7 \times 7) Surface. *Angew. Chem., Int. Ed.* **2000**, *39*, 2740–2743. (i) Tao, F.; Wang, Z. H.; Lai, Y. H.; Xu, G. Q. Attachment of Styrene and Phenylacetylene on Si(111)-7 \times 7: The Influence of Substitution Groups on The Reaction Mechanism and Formation of π -Conjugated Skeletons. *J. Am. Chem. Soc.* **2003**, *125*, 6687–6696. (j) Tao, F.; Wang, Z. H.; Chen, X. F.; Xu, G. Q. Selective Attachment of Benzonitrile on Si(111)-7 \times 7: Configuration, Selectivity, and Mechanism. *Phys. Rev. B* **2002**, *65*, 115311/1–9. (k) Yuan, Z. L.; Chen, X. F.; Wang, Z. H.; Yong, K. S.; Cao, Y.; Liu, Q. P.; Xu, G. Q. Dissociative Adsorption of Pyrrole on Si(111)-7 \times 7. *J. Chem. Phys.* **2003**, *119*, 10389–10395. (l) Tao, F.; Yuan, Z. L.; Chen, X. F.; Qiao, M. H.;

- Wang, Z. H.; Dai, Y. J.; Huang, H. G.; Cao, Y.; Xu, G. Q. Multiple Configurations of *N*-Methylpyrrole Binding on Si(111)-7 × 7. *Phys. Rev. B*, **2003**, *67*, 245406/1–8. (m) Tao, F.; Lai, Y. H.; Xu, G. Q. Si–C(N) σ Linkages and N → Si Dative Bonding at Pyridine/Si(111)-7 × 7. *Langmuir* **2004**, *20*, 366–368.
- (15) Riviere, J. C. *Surface Analytical Techniques*, Oxford University Press: New York, 1990.
- (16) (a) Yoshinobu, J.; Tsuda, H.; Onchi, M.; Nishijima, M. Interaction of Ethylene with The Si(111)-(7 × 7) Surface—A Vibrational Study. *Solid State Commun.* **1986**, *60*, 801–805. (b) Rehybridization of Acetylene on The Si(111)-(7 × 7) Surface—A Vibrational Study. *Chem. Phys. Lett.* **1986**, *130*, 170–174.
- (17) Piancastelli, M. N.; Motta, N.; Sgarlata, A.; Balzarotti, A.; Decresenzi, M. Topographic and Spectroscopic Analysis of Ethylene Adsorption on Si(111)-7 × 7 by STM and STS. *Phys. Rev. B* **1993**, *48*, 17892–17896.
- (18) Yoshinobu, J.; Fukushi, D.; Uda, M.; Nomura, E.; Aono, M. Acetylene Adsorption on Si(111)-(7 × 7)—A Scanning-Tunneling-Microscopy Study. *Phys. Rev. B* **1992**, *46*, 9520–9524.
- (19) Lu, X.; Lin, M. C. Reactions of Some [C,N,O]-Containing Molecules with Si Surfaces: Experimental and Theoretical Studies. *Int. Rev. Phys. Chem.* **2002**, *21*, 137–184.
- (20) Shachal, D.; Manassen, Y.; Ter-Ovanesyan, E. Role of Chain Length on the Surface Chemistry of Dienes Studied by Scanning Tunneling Microscopy. *Phys. Rev. B* **1997**, *55*, 9367–9370.
- (21) Jacox, M. E. Matrix-Isolation Study of the Interaction of Excited Argon Atoms with Methyl Cyanide—Vibrational and Electronic-Spectra of Ketenimine. *Chem. Phys.* **1979**, *43*, 157–172.
- (22) Hehre, W. J.; Yu, J.; Klunzinger, P. E.; Lou, L. *A Brief Guide to Molecular Mechanics and Quantum Chemical Calculation*. Wavefunction, Irvine, CA, 1998.
- (23) Hovis, J. S.; Coulter, S. K.; Hamers, R. J.; D'Evelyn, M. P.; Russell, J. N.; Butler, J. E. Cycloaddition Chemistry at Surfaces: Reaction of Alkenes with The Diamond(001)-2 × 1 Surface. *J. Am. Chem. Soc.* **2000**, *122*, 732–733.
- (24) Wang, G. T.; Bent, S. F.; Russell, J. N.; Butler, J. E.; D'Evelyn, M. P. Functionalization of Diamond(100) by Diels–Alder Chemistry. *J. Am. Chem. Soc.* **2000**, *122*, 744–745.
- (25) (a) Liu, Q.; Hoffmann, R. The Bare and Acetylene Chemisorbed Si(001) Surface and The Mechanism of Acetylene Chemisorption. *J. Am. Chem. Soc.* **1995**, *117*, 4082–4092. (b) Chadi, D. J. Atomic and Electronic-Structures of Reconstructed Si(100) Surfaces. *Phys. Rev. Lett.* **1979**, *43*, 43–47. (c) Hukka, T. I.; Pakkanen, T. A.; D'Evelyn, M. P. Chemisorption of Hydrogen on The Diamond (100)-2 × 1 Surface—An *ab-Initio* Study. *J. Phys. Chem.* **1994**, *98*, 12420–12430.
- (26) Lu, X.; Wang, X. L.; Yuan, Q. H.; Zhang, Q. Diradical Mechanisms for The Cycloaddition Reactions of 1,3-Butadiene, Benzene, Thiophene, Ethylene, and Acetylene on A Si(111)-7 × 7 Surface. *J. Am. Chem. Soc.* **2003**, *125*, 7923–7929.
- (27) Taguchi, Y.; Fujisawa, M.; Nishijima, M. Adsorbed State of Benzene on The Si(111)-7 × 7 Surface. *Chem. Phys. Lett.* **1991**, *178*, 363–368.
- (28) Sibi, M. P. Enantioselective Free Radical Reactions. *Acc. Chem. Res.* **1999**, *32*, 163–171.
- (29) Hawker, C. J. “Living” Free Radical Polymerization: A Unique Technique for The Preparation of Controlled Macromolecular Architectures. *Acc. Chem. Res.* **1997**, *30*, 373–382.
- (30) (a) Boland, J. J. The Importance of Structure and Bonding in Semiconductor Surface Chemistry: Hydrogen on the Si(111)-7 × 7 Surface. *Surf. Sci.* **1991**, *244*, 1–14. (b) Lo, R. L.; Ho, M. S.; Hwang, I. S.; Tsong, T. T. Diffusion by Bond Hopping of Hydrogen Atoms on the Si(111)-7 × 7 Surface. *Phys. Rev. B* **1998**, *58*, 9867–9875. (c) Vittadini, A.; Selloni, A. Binding Sites, Migration Paths, and Barriers for Hydrogen on Si(111)-7 × 7. *Phys. Rev. Lett.* **1995**, *75*, 4756–4759.
- (31) Cao, X. P.; Hamers, R. J. Silicon Surfaces as Electron Acceptors: Dative Bonding of Amines with Si(001) and Si(111) Surfaces. *J. Am. Chem. Soc.* **2001**, *123*, 10988–10996.
- (32) Lindberg, B. J.; Hedman, J. Molecular Spectroscopy by Means of ESCA 0.6. Group Shifts for N, P, and As Compounds. *Chem. Scr.* **1975**, *7*, 155–166.

AR0400488